World Electric Vehicle Journal

MDPI

Article

Ride Blending Control for Electric Vehicles

Vincenzo Ricciardi [1,*], Valentin Ivanov [1], Miguel Dhaens [2], Bert Vandersmissen [2], Marc Geraerts [2], Dzmitry Savitski [3] and Klaus Augsburg [1]

1 TU Ilmenau, Automotive Engineering Group, Ehrenbergstr. 15, 98693 Ilmenau, Germany; valentin.ivanov@tu-ilmenau.de (V.I.); klaus.augsburg@tu-ilmenau.de (K.A.)
2 Tenneco Automotive, Advanced Chassis Research, IZ A Schurhovenveld 1037, 3800 St Truiden, Belgium; MDhaens@Tenneco.com (M.D.); BVanders@tenneco.com (B.V.); MGeraerts@Tenneco.com (M.G.)
3 Arrival Germany GmbH, Core Components, Irma-Feldweg-Str. 8, 75179 Pforzheim, Germany; dzmitry.savitski@tu-ilmenau.de
* Correspondence: vincenzo.ricciardi@tu-ilmenau.de; Tel.: +49-3677-69-3843

Received: 18 April 2019; Accepted: 28 May 2019; Published: 31 May 2019

Abstract: Vehicles equipped with in-wheel motors (IWMs) feature advanced control functions that allow for enhanced vehicle dynamics and stability. However, these improvements occur to the detriment of ride comfort due to the increased unsprung mass. This study investigates the driving comfort enhancement in electric vehicles that can be achieved through blended control of IWMs and active suspensions (ASs). The term "ride blending", coined in a previous authors' work and herein retained, is proposed by analogy with the brake blending to identify the blended action of IWMs and ASs. In the present work, the superior performance of the ride blending control is demonstrated against several driving manoeuvres typically used for the evaluation of the ride quality. The effectiveness of the proposed ride blending control is confirmed by the improved key performance indexes associated with driving comfort and active safety. The simulation results refer to the comparison of the conventional sport utility vehicle (SUV) equipped with a passive suspension system and its electric version provided with ride blending control. The simulation analysis is conducted with an experimentally validated vehicle model in CarMaker® and MATLAB/Simulink co-simulation environment including high-fidelity vehicle subsystems models.

Keywords: in-wheel-motors; kinematics and compliance; driving comfort

1. Introduction

The use of in-wheel motors (IWMs) in fully electric vehicles (EVs) brings about several benefits, such as enhanced actuator response and brake regeneration, which results in improved driving safety and motion control. Nowadays, a number of well-established engineering solutions for these chassis control systems (e.g., torque vectoring and wheel slip control) are already available for serial EVs [1–3]. However, IWMs may also have an adverse effect on ride comfort due to the increased unsprung mass, which causes higher vibration, particularly in the 4–8 Hz range, where humans are more sensitive to vertical accelerations [4–6]. The effect of increased unsprung mass on ride comfort can be assessed through simulation analysis with the quarter-car model, where the road input is generated in accordance with ISO8606 [7]. The corresponding power spectral density of the heave acceleration is reported in the Figure 1 for the baseline case and the vehicle equipped with IWMs, respectively. In this analysis, the vehicle equipped with IWMs features a 50% increase of the unsprung mass for each wheel.

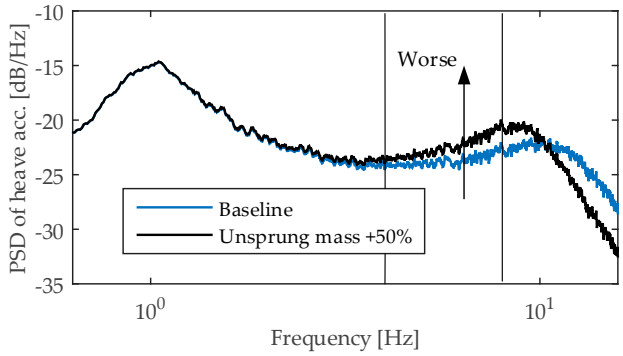

Figure 1. Effect of 50% increase in the unsprung mass on the vertical acceleration of vehicle body. The resultant worsening of ride comfort is reflected by higher Power Spectral Density in the frequency range 4–8 Hz, where the driver is more sensitive to vertical accelerations.

Several research instances investigated the effects of unsprung mass increase on the ride comfort. Anderson, Hurdwell, and Harty analyzed the impact that a 30 kg mass increase for each wheel has on the vehicle dynamics [6,8]. The results of this study demonstrated that such an increase of unsprung mass leads to the degradation of ride comfort in terms of pitch dynamics, impact feel on rough road, and agility. Another negative effect for some IWM design variants is that road excitations can lead to magnet gap deformation and, therefore, to magnetic force oscillations in the IWM [9]. As a result, the tuning of suspension design for EV with IWMs is required with consideration of the effect of reduced frequency of the wheel hop. The solution to install a stiffer suspension cannot be sufficient because this leads to a higher EV body acceleration. Additional boundaries in this case are also set by the tyre stiffness. These arguments show that a tuning of the passive suspension has a limited applicability to improve the ride quality of the EV with IWMs that was also confirmed by some research works [10]. These facts motivated further developments and studies for EV ride dynamics, which led to active ride control by means of IWM torque allocation.

This approach is based on the evidence that variations in the IWM torque allow for alteration of the wheel vertical force [11], whose magnitude depends on the suspension layout [12]. This effect can be exploited to reduce longitudinal vibrations [13–15], vehicle pitch during braking/acceleration [16–18], vehicle heave [19], and suppress the roll motion [20] when the lateral dynamics is excited. The mentioned effects were combined in Reference [21] to suppress sprung mid-frequency vibrations on heave, pitch and roll motion by utilisation of IWMs on the rear wheels. Nevertheless, the improvement of EV ride comfort trough targeted IWM torque modulation has also functional limitations.

An analysis of previous solutions shows that a reasonable advancement can be brought to the integration of the AS with the IWM-based ride dynamics control. This article focuses on the driving comfort enhancement by means of blended operation of IWMs and ASs. At the present stage of research, IWM control is utilised only for pitch motion control. Without loss of generality, a different force allocation on the two sides of the vehicle can be used to generate an anti-roll moment and, thus, suppress the roll motion. The term "ride blending", coined in a previous authors' work [22] and herein retained, is proposed by analogy with the brake blending, widely investigated in the research field related to EV. An experimentally validated model of a full electric sport utility vehicle (SUV), equipped with four IWMs, is used to investigate body's heave, roll, and pitch, and wheels' vertical motion. The vehicle model is based on the IPG CarMaker® simulation platform, whilst the vehicle subsystems are realised in MATLAB/Simulink environment. To this effect, data collected at Tenneco Automotive (Belgium) are used to validate a second order system dynamics, which reproduces the real transient response of the AS system and consider physical system constraints.

Hereunto, the effectiveness of the proposed controller is demonstrated with respect to the following test scenarios: straight line braking, sine sweep, and brake-in-turn (ISO 7975). The vehicle used for test

comparison is the same model SUV equipped with conventional internal combustion engine (ICE) and passive suspensions.

This work represents a follow-up research to the preliminary studies on ride blending presented at EVS31 conference in Kobe (Japan) with the paper titled "Ride Blending Control for Electric Vehicles" [22]. The previous work only provides a general introduction to the ride blending controller and vehicle modelling. In the present article, the model has been improved to consider complex manoeuvres and an assessment criteria based on the key performance indexes is put forth. In this study, a decentralised control architecture has been used due to its simplicity of implementation. However, the authors envisage that a centralized controller would be more suitable for the ride blending in the multi-actuated SUV equipped with four ASs and four IWMs. In the future, a sophisticated centralized controller will be implemented and benchmarked against the decentralized architecture.

The authors acknowledge that the information herein reported represents new advancements in the field of ride blending control and have not been dealt with previously. The paper is organized as follows. Section 2 puts forth the vehicle model and its subsystems. In Section 3, the decentralized architecture and control functions thereof are presented. Simulation results are reported in Section 4, which demonstrates the advantaged of the ride blending concept and the limitations of the decentralized control architecture. The performance of the AS with the IWM-based ride dynamics control is compared with the conventional passive suspension system. The enhancement in ride performance is reflected by improvement in key performance indexes (KPI) associated with driving comfort and active safety [6].

2. Vehicle Model

2.1. Vehicle Subsystems

The vehicle under investigation is a SUV equipped with electro hydraulic brake (EHB) system, an electric powertrain with four IWMs and hydraulic ASs. A schematic of the research item is reported in the Figure 2. The parametrized vehicle model has been validated against experimental data collected at the Technische Universität Ilmenau (TU Ilmenau) and implemented in the proprietary software IPG CarMaker®. The wheel force data from vehicle testing on proving ground and tyre test rig were exploited to validate the Magic formula [23]. The electric motors are included in the vehicle dynamics simulation software under the form of torque and efficiency maps, whilst a first order transfer function describes their transient response.

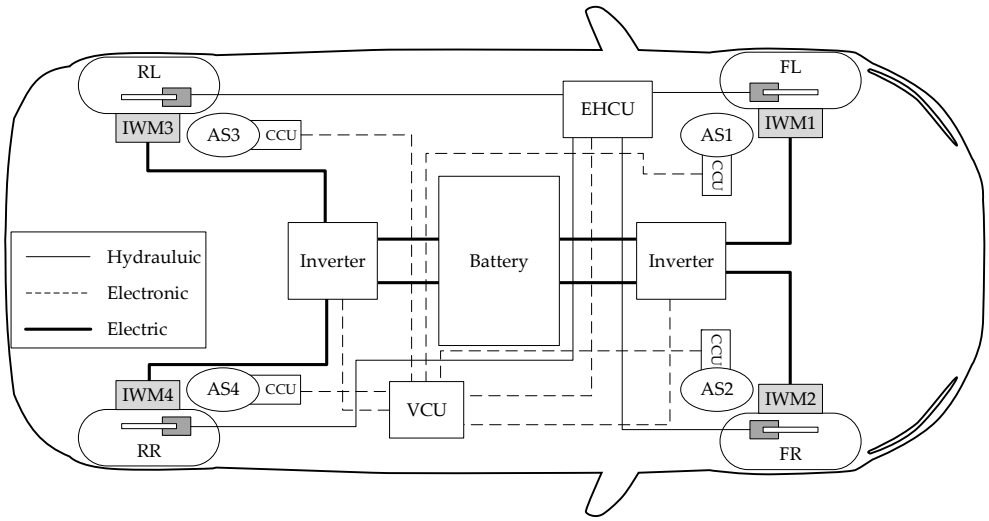

Figure 2. Configuration of the full electric vehicle under analysis. IWM—In-wheel motor; AS—Active suspension; CCU—Corner control unit; EHCU—Electrohydraulic control unit; VCU—Vehicle control unit.

In the present analysis, the EHB is deactivated and the braking is realized by full use of IWMs, namely full regenerative braking. The employed IWMs can deliver a peak torque of 600 Nm at a maximum speed of 1500 rpm. The AS system considered in this study is of hydraulic type (Figure 3). The ACOCAR® hydraulic AS is comprised of an actuator, an electrohydraulic control valve, and a pump. Due to the placement of a suspension system at each corner of the vehicle, the anti-roll bars on front and rear axles are not required. The specifications of this system are determined based on measurements performed at Tenneco Automotive, Belgium. The dynamics of the hydraulic actuator is taken into account by means of a second order transfer function.

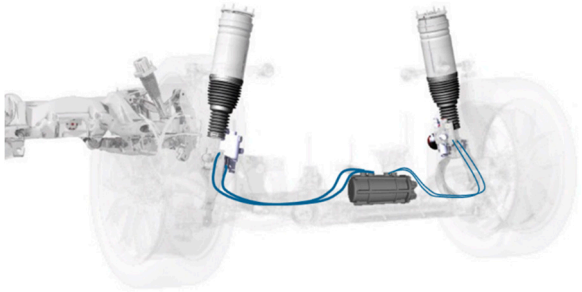

Figure 3. Depiction of the ACOCAR® hydraulic active suspension system (Tenneco Automotive).

2.2. Suspension Kinematics and Compliance

The geometry of the vehicle roll and pitch motions in accordance with the experimentally validated vehicle model is reported in the Figure 4. The suspensions' kinematics and compliance (K&C) is modelled and parametrized accordingly. As IWMs are installed below the suspension, a force with vertical direction is generated as the electric motors are actuated (see Figure 4, right). To this effect, the vehicle dynamics simulation software accounts for variations in the swing arm instantaneous centre of front and rear suspensions, which stem from the combined effect of body inertial forces and vertical wheel forces. The knowledge of the swing arm instantaneous centre enables the evaluation of the vehicle pitching and roll characteristics and, thus, for a proper anti-dive/lift and anti-roll control of front and rear suspensions. The instantaneous pitch/roll centres are determined by intersecting the lines drawn from the tyre contact points to the swing arm instantaneous centre of rotation. In accordance with the suspensions kinematics of the employed vehicle, the swing arm centre position is a function of the relative wheel travel with respect to the vehicle body. Figure 5 reports the result of the SPMM (Suspension Parameter Measurement Machine) compliance testing for the vehicle under analysis. Data are hidden for privacy reasons. The proper design of front and rear swing arm centre positions is important to reduce pitch and roll by generating anti-dive (when braking), anti-squat (when accelerating), and anti-roll (when turning) forces.

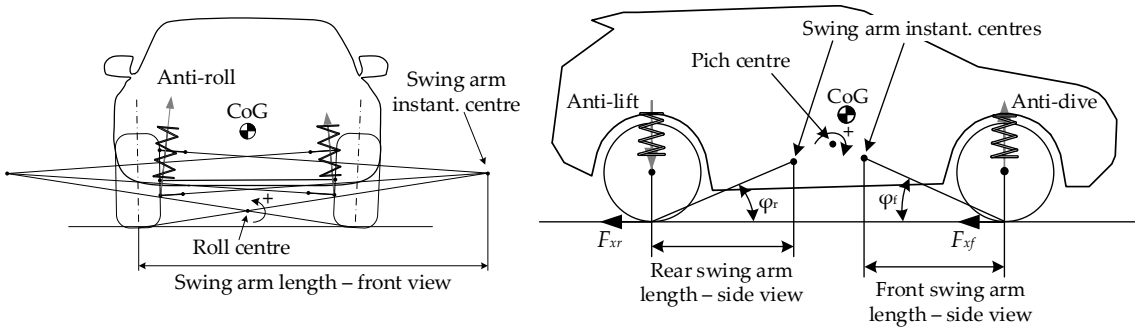

Figure 4. Front and side views of the experimentally validated vehicle model. The grey arrows represent the anti-roll and anti-dive/lift force generated by in-wheel motor (IWM) torque control to suppress the roll and pitch motion, respectively.

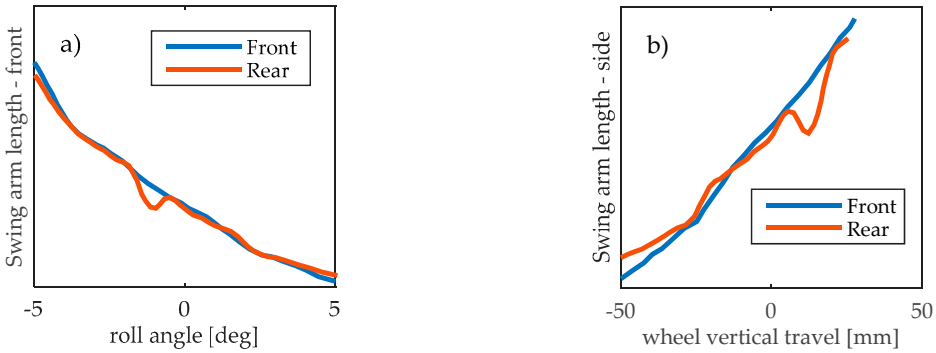

Figure 5. Partial Suspension Parameter Measurement Machine (SPMM) kinematics and compliance (K&C) test results: on the left, variation of the swing arm roll instant, centre position for the front-right and rear-right suspensions with respect to the relative body roll (the left side is omitted for sake of space). On the right, variation of the swing arm pitch instant. centres position for front and rear suspensions with respect to the vertical wheel translation. Values on Y-axis are omitted due to confidentiality.

3. Ride Blending Control

The proposed ride blending architecture is depicted in Figure 6. This latter is based on the principle of decentralized control, which at this stage of research represents a good compromise between ease of implementation and control performance.

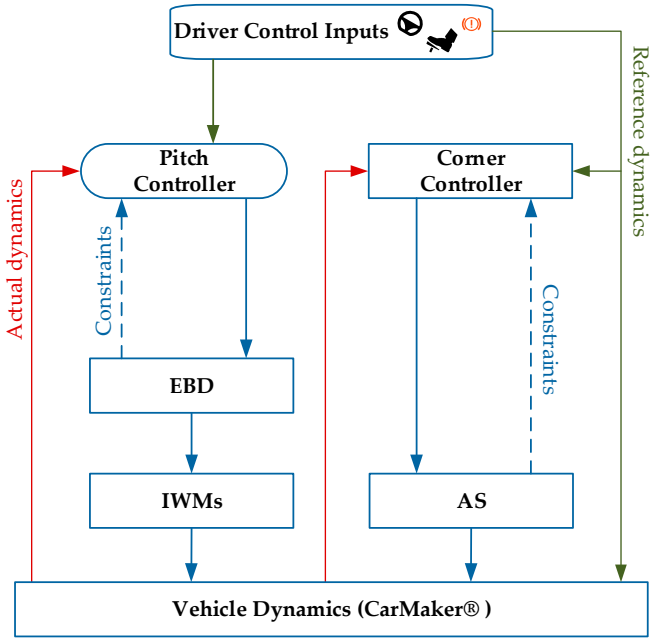

Figure 6. Ride blending control architecture. The control architecture features the in-wheel motors (IWMs) Pitch Controller serving the Electronic Brake Distribution (EBD) and the Corner Controller.

The "Pitch Controller" computes the reference states of the vehicle body dynamics for given manoeuvre conditions based on the "Driver Control Inputs", as the positions of the acceleration and brake pedals. The mentioned reference states, which are sent to the electronic brake distribution (EBD), are at this stage of the research related to the pitch motion, as will be explained in the next section. The Corner Controller depends on the applied ride control targets, which are related to one or more tasks, as road holding, handling, pitch control, heave control, etc. The reference states are compared with the actual states of the vehicle body dynamics provided by the vehicle on-board sensors and state estimators. EBD and the Corner Controller set up the control current for IWMs and actuators of the ASs. They produce required wheel torques and vertical forces correspondingly. The system

acts so that the control effort required from the Corner Controller is minimized once the EBD for minimum pitch intervenes. However, the limitations of this control algorithm will be discussed later on. The "Pitch Controller" and "Corner Controller" are based on the Proportional Integral (PI) controller, whose gains have been identified by analysing the frequency response for the closed-loop system of the driver vertical acceleration and angular rotations with varying vertical load and road input.

3.1. Electronic Brake Distribution (EBD) for Minimum Pitch

Brake proportioning is widely addressed in vehicle longitudinal dynamics to determine the brake force distribution between front and rear wheels without causing rear wheels to lock. While braking/accelerating or negotiating a turn, the vehicle is subject to a mass transfer that leads to a variation in the vertical load acting on a wheel. This leads to vehicle pitch and roll and, as a result, the vehicle driving comfort decreases. Vehicles equipped with IWMs can use the suspension reaction force generated by motor drive as a form of AS control [12]. At the present stage of research, the differential EBD is utilized only for pitch motion control.

By controlling the magnitude of the motor torque provided to each wheel, the anti-dive/lift force can be used for pitch motion suppression. In fact, load transfer can occur not only during vehicle acceleration/deceleration but also because of the anti-dive/lift forces brought about by the IWM architecture. Relevant to this study is the definition of ideal force distribution, based on which front and rear wheels exhibit the same tyre–road friction utilization [24]. The ideal force distribution against the braking acceleration demand is depicted in Figure 7. A control parameter $f \in R^+ : f_{min} < f < f_{max}$ is defined so that:

$$F_{xf} = F_{xf}^{ideal} + F_{xr}^{ideal} \cdot (1 - f) \tag{1}$$

$$F_{xr} = F_{xr}^{ideal} \cdot f \tag{2}$$

where, F_{xf}^{ideal} and F_{xr}^{ideal} are the longitudinal forces exerted by the front and rear wheels, respectively. The boundaries of the control parameter are reported in Figure 7, where the upper limit account for tyre-road friction utilisation on dry road and the lower limit complies the Regulation 13 ECE [25]. These constraints set the limits to avoid the rear wheels lock during braking. A control parameter equal to one means that the torque distribution is realized in accordance with the ideal curve. The "Pitch Controller" selects the control target to suppress the pitch motion by simultaneously ensuring the demanded acceleration/braking performance. Thereafter, the signal is processed by the EBD, which in turn actuates the IWMs.

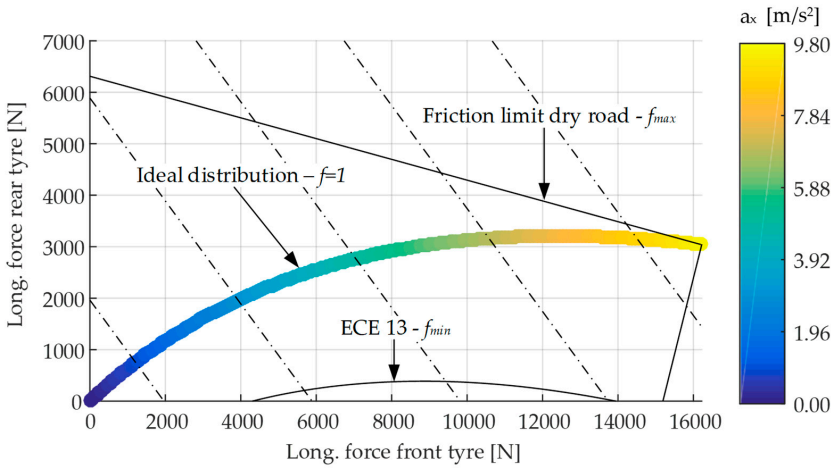

Figure 7. The figure shows the ideal braking force distribution, whereby the colorbar refers to the specific deceleration levels. The figure also reports the limit set by the R13 ECE (Economic Commission for Europe) [25] and the friction utilisation limit on dry road. Iso-deceleration conditions are represented by dash-dotted lines.

The same strategy is applied in the case of acceleration but it is here omitted for the sake of space. This strategy ensures that the pitch angle is reduced whilst the driver request is preserved.

3.2. Corner Controller

The corner controller employs the information of body pitch angle (ϑ), roll angle (φ), and heave displacement (z_s) to estimate the position of the suspension top-mount point $\left(z_{fl}, z_{fr}, z_{rl}, z_{rr}\right)$. Thereafter, the controller acts to minimize the acceleration of the top-mount positions, which results in an improved driving comfort. To this effect, the estimator requires the values of instantaneous pitch and roll centres positions, which are computed in accordance with the kinematics of the vehicle model depicted in Figure 8.

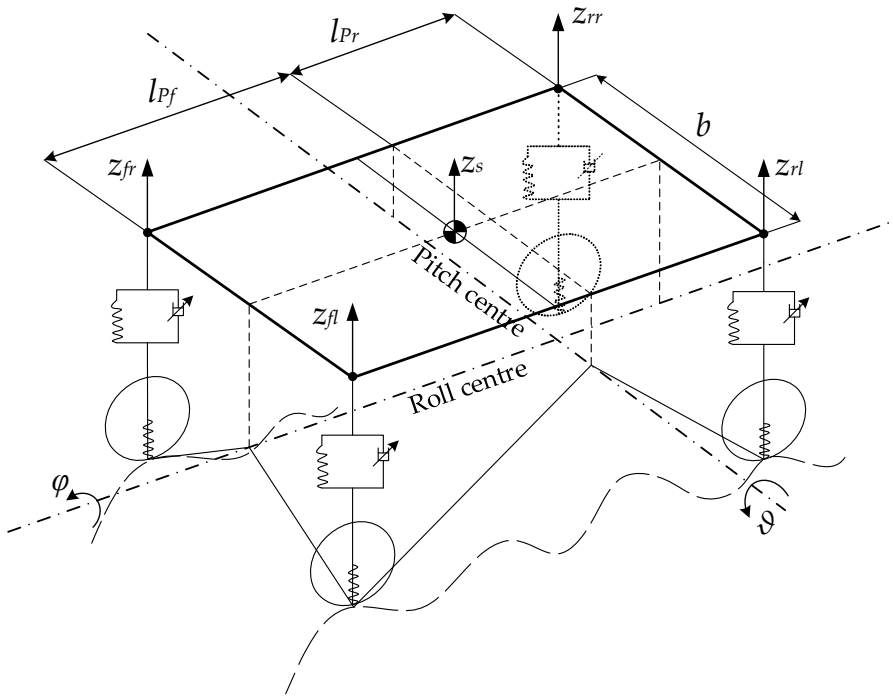

Figure 8. Schematic of the utilized vehicle model. Roll and pitch centre kinematics is relevant to the estimation of the suspension top-mount positions.

For small displacements and rotations, the following set of equations holds:

$$\begin{aligned} z_{fl} &= z_s + \varphi \cdot \tfrac{b}{2} - \vartheta \cdot l_{Pf}, \\ z_{fr} &= z_s - \varphi \cdot \tfrac{b}{2} - \vartheta \cdot l_{Pf}, \\ z_{rl} &= z_s + \varphi \cdot \tfrac{b}{2} + \vartheta \cdot l_{Pr}, \\ z_{rr} &= z_s - \varphi \cdot \tfrac{b}{2} + \vartheta \cdot l_{Pr}, \end{aligned} \tag{3}$$

where, b is the wheel track and l_{Pf} and l_{Pr} represent the distance of the pitch centre from the front and rear wheel centre, respectively. Hence, the control input acts to suppress the acceleration of the top-mount points. Given the linearity of the problem (3), this control provides a simultaneous abatement of heave, pitch, and roll motion.

4. Simulations

The proposed ride blending architecture was implemented in the proprietary vehicle dynamics simulation software IPG CarMaker®, which includes aerodynamic forces, non-linear suspension model, non-linear IWMs model, a complex model of the electrohydraulic brake system, and steering

system. The experimentally validated SUV-class vehicle and tyre Magic formula [23] were used during the simulations. The characteristics of the vehicle are reported in the Table 1.

Table 1. Vehicle Parameters.

Vehicle Type	SUV-Class Electric Vehicle	**Powertrain Type**	All-wheel drive
Front Semi-Wheelbase	1.104 m	**Drivetrain Type**	In-wheel motors
Rear Semi-Wheelbase	1.558 m	**Electric Motors**	Peak power 75 kW / Max speed 1500 rpm
CoG Height	0.644 m	**Suspension Type**	Hydraulic active
Vehicle Mass	1937 kg	**Tyre Size**	235/55 R19
Vehicle Track	1.613 m	**Brake System**	Combined electrohydraulic and regenerative system

The full electric SUV equipped with enabled ride blending is compared against its ICE counterpart, characterized by a lower unsprung mass. Three simulations are performed to assess the effectiveness of the proposed controller, namely the straight line braking, the sine sweep test, and the brake-in-turn (ISO 7975). The effectiveness of the proposed controller is enumerated by KPI associated with driving comfort and active safety. The driving comfort indexes are herein related to the RMS of the heave, pitch, and roll accelerations, respectively. The active safety is reflected by the RMS of the wheel vertical load variations, which have a detrimental effect on the tyre grip. The KPI are defined so that higher values correspond to better or safer performance. For the sake of clarity, the KPI are normalized with respect to the technology that achieve the highest score in terms of pitch, roll, heave suppression, and road holding.

4.1. Straight Line Braking

In the first scenario, the vehicle starts from an initial speed of 100 km/h and performs three consecutive braking manoeuvres until a stand still. The results of this simulation are reported in the Figure 9 and refer to three configurations, namely: the conventional SUV with passive suspension system (referred to as "Passive"), the full electric SUV equipped with ASs (also referred to as "AS" in the figure) and the upgraded configuration with ride blending control (referred to as "Ride Blending"). It is worth remarking that the controller preserves the same braking performance, achieving a pitch reduction without affecting the braking distance.

It is worth pointing out that superior performance in terms of pitch motion suppression can be achieved through blended action of IWM torque control and ASs (referred to as Ride Blend. in the figures). Indeed, the peak acceleration value is dramatically abated thanks to the braking torque distribution for minimum pitch. The results are confirmed by the KPI reported in the Figure 10. The KPI related to the roll motion is omitted because the associated dynamics is not excited during this test.

The results suggest that the ride blending control leads to improved pitch comfort with no deterioration of road holding. However, the EBD for minimum pitch has a detrimental effect on the vehicle heave as per Figure 10.

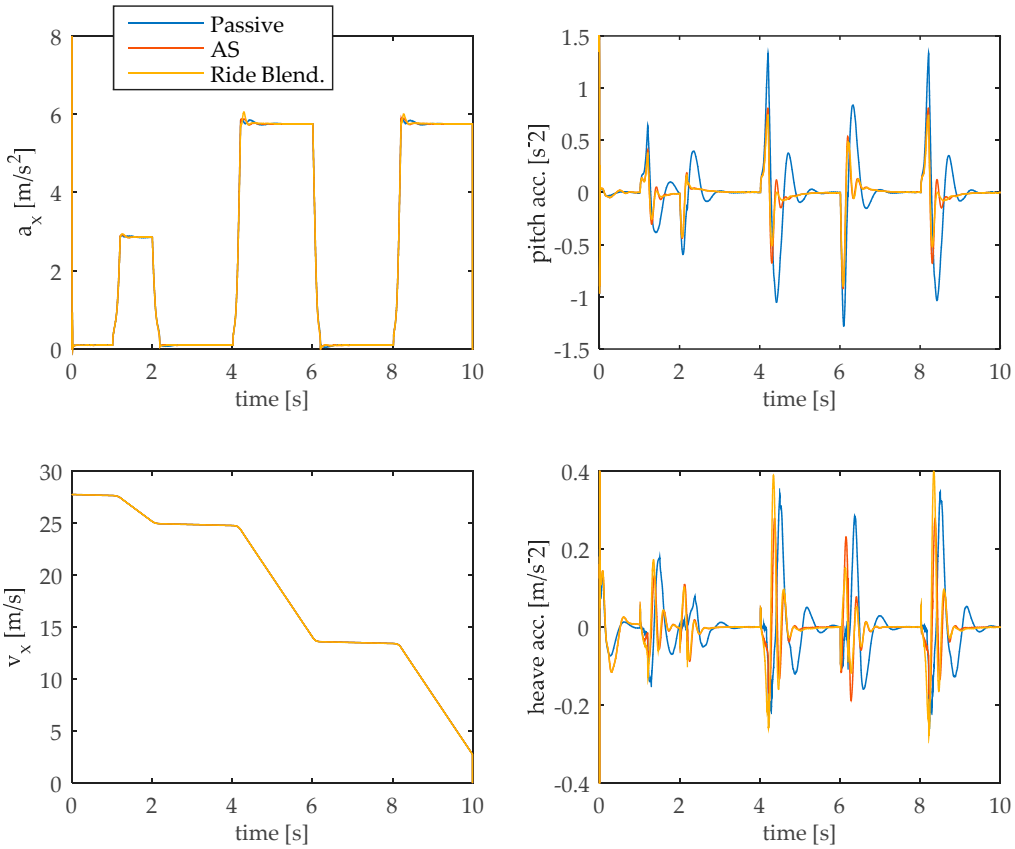

Figure 9. Simulation results for the straight line braking involving three consecutive brake pedal actuations.

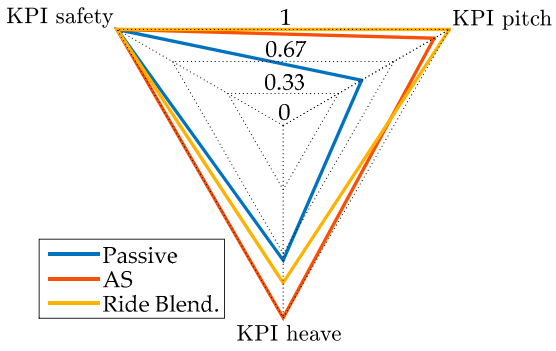

Figure 10. Key performance indexes improvement for the straight line braking maneuverer.

4.2. Sweep Test

The second test involves a constant driving speed of 50km/h and a sinusoidal steering input. The swept sine test is performed to quantify the vehicle handling response to a steer input that covers a wide range of frequencies, namely from 1 Hz to 5 Hz. Figure 11 shows the performance of roll and heave for the sine sweep test. For this test, the ride blending corresponds to the AS control, as the EBD for minimum pitch is disabled due to limited pitch motion. The AS control improves the roll motion for the whole frequency spectrum guaranteeing the driving performance.

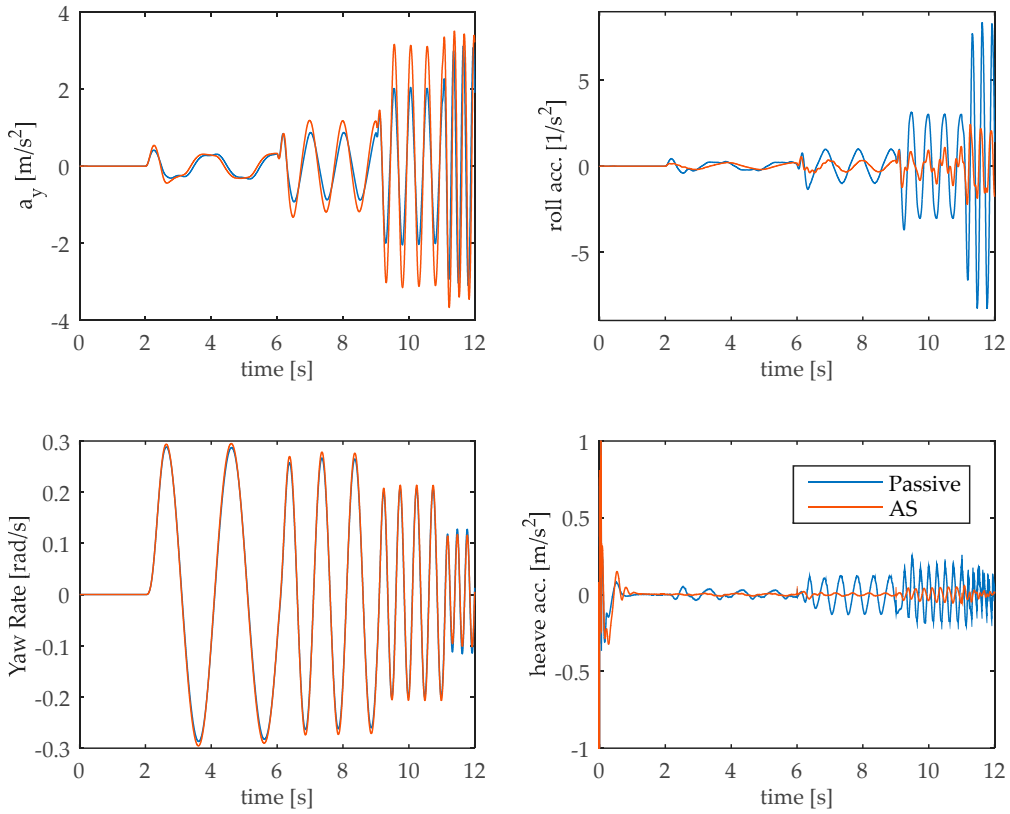

Figure 11. Simulation results for the sweep test. The graphs on the left side show the vehicle lateral acceleration and yaw rate, respectively. The graphs on the right side show the roll and heave acceleration, respectively.

The enhanced performance is confirmed by the increased KPI in Figure 12. Such analysis supports the previous statement and confirms that the AS control increases the driving comfort. The KPI related to the pitch motion is omitted because the associated dynamics are not excited in this test.

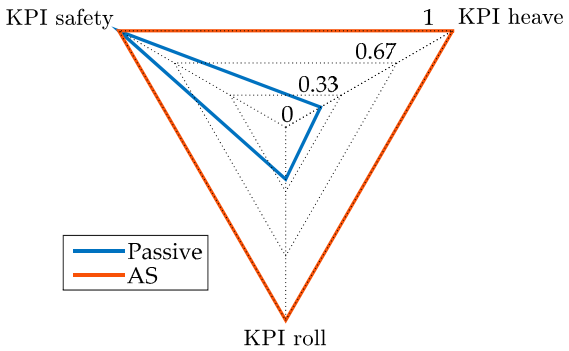

Figure 12. Key performance indexes improvement for the sine sweep test. The hydraulic active suspension (AS) allows for improved driving comfort with simultaneous preservation of the active safety requirements.

4.3. Brake-In-Turn (ISO 7975)

The last manoeuvres pertain to closed-loop brake-in-turn simulation on a dry road to investigate the effectiveness of the proposed ride blending controller when all the dynamics are excited. The performed simulation is based on ISO 7975 standard. The simulation results are reported in Figure 13. For a matter of clarity, the diagrams are limited to the time span where the brake-in-turn occurs.

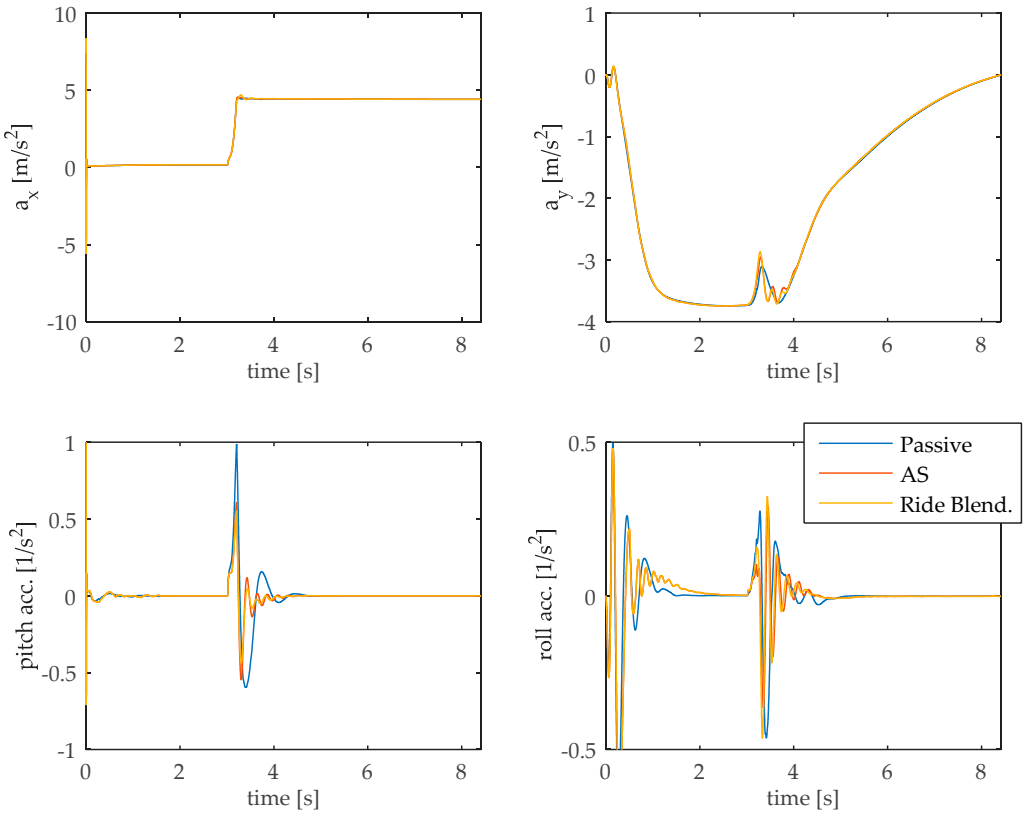

Figure 13. Simulation results for the ISO 7975 brake-in-turn. The upper graphs represent the longitudinal and lateral acceleration, respectively. The lower graphs show the resulting pitch and roll acceleration are reported.

The upper-left graph proves that the proposed controller does not affect the driving performance. The suppression of roll, pitch, and heave motion proves the superior performance of the proposed AS controller. The KPIs for the brake-in-turn are reported in the Figure 14.

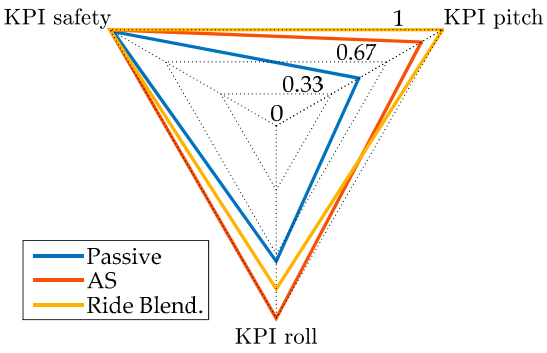

Figure 14. Key performance indexes for the brake-in-turn test. The electronic brake distribution (EBD) for minimum pitch improves the pitch motion to the detriment of the roll dynamics.

The strong pitch and roll dynamics caused by this test emphasize the limitations of the decentralized controller. Although the decentralized Ride Blending control offers benefits in terms of pitch control, it has a detrimental effect on the roll motion. Indeed, the implemented decentralized controller is not able to account for the coupled dynamics of pitch and roll when it comes to the combined brake-in-turn manoeuvre. The authors envisage that a more sophisticated centralized controller will be able to deal with this issue. Nevertheless, as for the previous tests, the ride blending has no detrimental effect of the road holding performance.

5. Conclusions

This work deals with the combined use of IWM torque control and AS to suppress the pitch, roll, and heave motion. An experimentally validated model of SUV with four IWMs has been used in the proprietary vehicle dynamics simulator IPG CarMaker®. The control performances are analyzed with reference to the straight line braking, the sine sweep test, and the brake-in-turn (ISO 7975). A previous authors' work demonstrated that the proposed ride blending control suppresses the pitch and roll motion for the whole frequency spectrum between 1 Hz and 8 Hz [22], where the driver is more sensitive to vibration. In this work, the effectiveness of the proposed ride blending control is confirmed by the improved KPIs. The brake-in-turn brings out the limitation of the decentralized controller, as the blended action of the Pitch Controller reduces the control effort on the Corner Controller to the detriment of the roll motion. Overall, despite an increase in the unpsrung mass leads to degraded road holding and higher vibration, the results demonstrate that the proposed ride blending allows for an improved driving comfort without degradation of active safety. Subsequent studies will account for the differential torque allocation on the vehicle's left and right sides to suppress the roll motion by IWM control. To this effect, a more complex architecture based on the centralized control will be developed, whereby the control allocation for the multi-actuated SUV will be realised with respect to criteria of energy optimization and riding comfort.

Author Contributions: The authorship is limited to those who have contributed substantially to the work realisation. All the authors have participated to the design of experiments, analysis of data and results, and writing of the paper.

Funding: This work is supported by the European Union Horizon 2020 Framework Program, Marie Skłodowska-Curie actions, under grant agreement no. 734832. Further activities are also being performed under support of the project A-MOTION funded by the German Federal Ministry for Education and Research.

Conflicts of Interest: The authors declare no conflict of interest.

References

1. Novellis, L.D.; Sorniotti, A.; Gruber, P.; Shead, L.; Ivanov, V.; Hoepping, K. Torque vectoring for electric vehicles with individually controlled motors: State-of-the-art and future developments. *World Electr. Veh. J.* **2012**, *5*, 617–628. [CrossRef]
2. Ivanov, V.; Savistki, D.; Shyrokau, B. A survey of traction control and antilock braking systems of full electric vehicles with individually controlled electric motors. *IEEE Trans. Veh. Technol.* **2014**, *64*, 3878–3896. [CrossRef]
3. Shuai, Z.; Zhang, H.; Wang, J.; Li, J.; Ouyang, M. Combined AFS and DYC control of four-wheel-independent-drive electric vehicles over CAN network with time-varying delays. *IEEE Trans. Veh. Technol.* **2013**, *63*, 591–602. [CrossRef]
4. *Guide to the Evaluation of Human Exposure to Whole Body Vibration—Part 2: Vibration in Buildings*; ISO 2631-2; International Organization for Standardization: Geneva, Switzerland, 2003.
5. Society of Automotive Engineers of Japan. *Automotive Technology Handbook 1, Introduction/Theory*; Society of Automotive Engineers of Japan: Tokyo, Japan, 1990; p. 269.
6. Anderson, M.; Harty, D. Unsprung Mass with In-wheel Motors—Myths and Realities. *Proc. AVEC* **2010**, *10*, 261.
7. International Organization for Standardization. *Mechanical Vibration-Road Surface Profiles-Reporting of Measured Data*; ISO 8606 (1995); International Organization for Standardization: Geneva, Switzerland, 1995.
8. Hurdwell, R.; Anderson, M. *Dynamics of Vehicles with In-Wheel Motors*; Cambridge University: Cambridge, UK, 2011.
9. Luo, J.; Tan, D. Study on Dynamics of the In-Wheel Motor System. *IEEE Trans. Veh. Technol.* **2012**, *61*, 3510–3518.
10. Rohas, A.; Niderkofler, H.; Willberger, J. Comfort and Safety Enhancement of Passenger Vehicles with In-Wheel Motors. *SAE Technical Paper*, 12 April 2010. [CrossRef]

11. Murata, S. Vehicle dynamics innovation with in-wheel motor (No. 2011-39-7204). *SAE Technical Paper*, 17 May 2011.
12. Katsuyama, E. Decoupled 3D Moment Control for Vehicle Motion Using In-Wheel Motors. *SAE Int. J. Passeng. Cars-Mech. Syst.* **2010**, *6*, 137–146. [CrossRef]
13. Fukudome, H. Reduction of Longitudinal Vibration Using In-Wheel Motors. *Trans. Soc. Automot. Eng. Jpn.* **2016**, *47*, 457–462.
14. Savitski, D.; Ivanov, V.; Augsburg, K.; Shyrokau, B.; Wragge-Morley, R.; Pütz, T.; Barber, P. The new paradigm of an anti-lock braking system for a full electric vehicle: Experimental investigation and benchmarking. *Proc. Inst. Mech. Eng. Part D J. Automob. Eng.* **2016**, *230*, 1364–1377. [CrossRef]
15. Savitski, D.; Ivanov, V.; Shyrokau, B.; Pütz, T.; De Smet, J.; Theunissen, J. Experimental investigations on continuous regenerative anti-lock braking system of full electric vehicle. *Int. J. Automot. Technol.* **2016**, *17*, 327–338. [CrossRef]
16. Tavernini, D.; Velenis, E.; Longo, S. Feedback brake distribution control for minimum pitch. *Veh. Syst. Dyn.* **2017**, *55*, 902–923. [CrossRef]
17. Kanchwala, H.; Wideberg, J. Pitch reduction and traction enhancement of an EV by real-time brake biasing and in-wheel motor torque control. *Int. J. Veh. Syst. Model. Test.* **2016**, *11*, 165–192. [CrossRef]
18. Qu, T.; Fujimoto, H.; Hori, Y. Pitch Motion Control without Braking Distance Extension considering Load Transfer for Electric Vehicles with In-Wheel Motors. *IEE-Jpn. Tech. Meet. Rec.* **2012**, *IIC-12-104*, 105–110.
19. Kamiya, N.; Fujimoto, H.; Hori, Y.; Katsuyama, E.; Kanou, T. Reduction of Vertical Vibration for Improvement of Ride Comfort Using In-Wheel Motors. In Proceedings of the IEE-Japan Industry Application Society Conference (JIASC), Hakodate, Japan, 29–31 August 2017.
20. Kawashima, K.; Uchida, T.; Hori, Y. Rolling stability control of in-wheel electric vehicle based on two-degree-of-freedom control. In Proceedings of the 2008 10th IEEE International Workshop on Advanced Motion Control, Trento, Italy, 26–28 March 2008.
21. Katsuyama, E.; Omae, A. Improvement of Ride Comfort by Unsprung Negative Skyhook Damper Control Using In-Wheel Motors. *SAE Int. J. Altern. Powertrains* **2016**, *5*, 214–221. [CrossRef]
22. Ivanov, V.; Dhaens, M.; Ricciardi, V.; Savitski, D.; Augsburg, K. Ride Blending Control for Electric Vehicles. In Proceedings of the 31st International Electric Vehicles Symposium & Exhibition (EVS 31), Kobe, Japan, 30 September–3 October 2018.
23. Pacejka, H.B. *Tire and Vehicle Dynamics*, 3rd ed.; Butterworth-Heinemann: Oxford, UK, 2012.
24. Pennycott, A.; De Novellis, L.; Gruber, P.; Sorniotti, A. Optimal braking force allocation for a four-wheel drive fully electric vehicle. *Proc. Inst. Mech. Eng. Part I J. Syst Control Eng.* **2014**, *228*, 621–628. [CrossRef]
25. Economic Commission for Europe. *Uniform Provisions Concerning the Approval of Vehicles of Categories M, N and O with Regard to Braking. Addendum 12: Regulation No. 13*; Economic Commission for Europe: Geneva, Switzerland, 2008.